Pergamon

Int. J. Solids Structures Vol. 31, No. 6, pp. 865–889, 1994
Elsevier Science Ltd
Printed in Great Britain
0020–7683/94 $6.00 + .00

A NUMERICAL STUDY OF STRESS SINGULARITIES IN A TWO-MATERIAL WEDGE

L. GU and T. BELYTSCHKO
Department of Civil Engineering, Robert R. McCormick School of Engineering and Applied Science, The Technological Institute, Northwestern University, Evanston IL 60208-3109, U.S.A.

(*Received* 2 *January* 1993; *in revised form* 8 *September* 1993)

Abstract—A general numerical procedure for determining the stress singularity at the vertex of a two material wedge is presented. Using an eigenfunction expansion technique and assuming the asymptotic displacement field or stress potential to be of the form $r^{\lambda}F(\theta)$, a finite element approach is constructed. The dominant order of stress singularity is determined by solving the eigenvalue equation obtained from the finite element model. Numerical results for some specific problems are given. These results include the order of stress singularities at the free edge of an interface between adjacent layers in a laminated composite, as well as the case of an interface crack in a composite laminate. Results are also obtained by a spectral overlay on a finite element mesh through a least square procedure and show that if high resolution is used near the free edge, a good estimate of singularity can be obtained.

1. INTRODUCTION

Interface cracks have been an intense subject of research during the past 30 years. A variety of analytical tools has been developed for determining the strength of stress singularities at the crack tip. For the problem of an interface crack between dissimilar isotropic materials, several elastic solutions have been given. Williams (1959), and later Rice and Sih (1965) investigated the singular field ahead of the crack and found that the stresses exhibit an oscillatory solution. Erdogan (1965), England (1965), Dundurs (1969) and Comninou (1977) gave solutions of some specific interface crack problems.

Interface cracks between two anisotropic materials have also been studied. Goton (1967), Clements (1971), Willis (1971), and Wang and Choi (1983) presented elastic solutions which exhibit an oscillatory stress singularity at the interface crack tip between anisotropic materials.

Renewed interest in this field occurred due to interest in the mechanical behavior at free edges of laminated composites, a problem unique to composite laminates and not observed in homogeneous solids in general. Because of its complexities, an analytical method to obtain a complete solution seems impossible. However, several approximate numerical solutions for the problem of finite-width laminates subjected to uniform axial strain are available. These results show good agreement for the points away from the free edge. For the points near the free edge, the stresses obtained by various investigators disagree with each other.

The first approximate solution of interlaminar stresses was proposed by Pipes and Pagano (1970), who used an elastic, quasi-three-dimensional solution by finite difference techniques to evaluate interlaminar stresses. The results showed that the stress states exhibit high gradients and perhaps singularities along the free edges of the laminates. A large variety of numerical methods has been proposed to calculate interlaminar stress. The representative methods include: the finite difference method by Pipes and Pagano (1970), boundary-layer theory by Tang and Levy (1975), perturbation methods by Hsu and Herakovich (1977), series solutions by Wang and Dickson (1978) and finite element methods by Wang and Crossman (1977), Herakovich *et al.* (1979), Spilker and Chou (1980), Raju and Crews (1981), Hsiao (1991) and Gu and Reddy (1992). Excellent reviews on this field are available (Whitecomb *et al.*, 1982; Ye, 1990; Gu and Reddy, 1992).

Pipes and Pagano (1970) suggested from their finite difference results that there might be a singularity in the distributions of interlaminar stresses at the corner of the free edge

interface. The finite element results by Wang and Crossman (1977) and later by Raju and Crews (1981) appeared to confirm the existence of a stress singularity at the intersection of the interface and free edge, and the singularity of the interlaminar stresses then became the focus of attention. Wang and Choi (1982) and Zwiers *et al.* (1982), separately, obtained the strengths of the singularity through the complex-variable method.

Although analytical methods have been used to examine the stress singularity in the two material wedge, very few numerical methods with more complete results have been developed. Some numerical methods have been developed for other singular problems. Using an eigenfunction expansion technique for the displacement field, Bazant and Estenssord (1979) and Somaratna and Ting (1986) developed a finite element method to determine the three-dimensional crack singularities. Barsoum (1988, 1990) used an iterative finite element method for the eigenvalue problem of a crack between dissimilar isotropic media to determine the strength of the stress singularity. However, no numerical solutions are available for the singularities in the Pipes and Pagano problem or for the interface crack between two anisotropic materials.

In the present study, we first investigate the use of a spectral overlay finite element method which was developed by Belytschko *et al.* (1990) and Belytschko and Lu (1992) for solving the edge-stress problem. Following the discussion of the stress singularity in the composite laminates, a numerical approach for determining the stress singularities in a two material wedge is developed and applied to the study of free-edge and interface crack problems. Two methods for deriving the finite element formulation are used:

(1) a method based on a stress function;
(2) a method based on the interpolation of displacements.

In the methods, quadratic and quartic eigenvalue problems are obtained, respectively.

The basic idea of our method is to assume that the strength of the stress singularity is dependent on the near field homogeneous solution, which admits a separable form. Following the derivation of the finite element formulation for the problems, some numerical results for special geometry in isotropic and anisotropic materials are presented and compared to analytical solutions.

It is observed that the method using quadratic (method 1) and linear (method 2) elements here is quite efficient in providing rapidly converging and accurate results. Several new examples are also given and discussed. These results deal with three areas for both isotropic and anisotropic materials: the interface crack, the wedge problem and the free edge effect.

2. THE SPECTRAL OVERLAY FINITE ELEMENT ANALYSIS OF STRESSES IN COMPOSITE LAMINATES

Laminate model

The problem considered is the uniaxial loading of a symmetric composite laminate. A typical laminate and the co-ordinate system are shown in Fig. 1. Each layer of the composite lies in a plane parallel to the (x, y) plane and is a fiber-reinforced composite material in which the fiber direction makes an angle α with x-coordinate. The laminate is assumed to

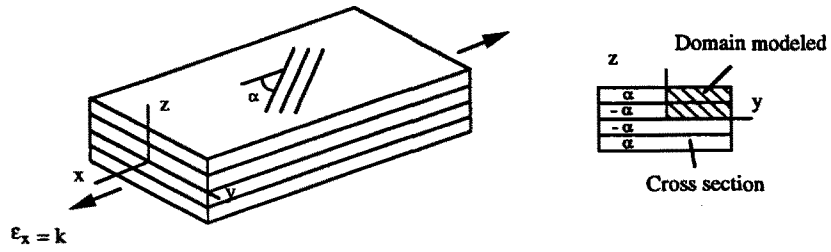

Fig. 1. Laminate geometry and loading.

be sufficiently long so that the end effect is neglected in the region far from the ends. Consequently, the stress state in the composite laminate is independent of the x-variable. Small deformation and an initially stress-free field with negligible body force are also assumed. With these assumptions, a pseudo three-dimensional displacement field can be written in the form (Pipes and Pagano, 1970):

$$u = kx + U(y, z), \tag{1}$$

$$v = V(y, z), \tag{2}$$

$$w = W(y, z), \tag{3}$$

where u, v and w are the displacements in x-, y- and z-directions, respectively, and k is the applied uniform axial strain.

The strain vector $\boldsymbol{\varepsilon}$ has the form:

$$\boldsymbol{\varepsilon}^T = \{\varepsilon_x \ \varepsilon_y \ \varepsilon_z \ \gamma_{yz} \ \gamma_{zx} \ \gamma_{xy}\} = \left\{k \ \frac{\partial v}{\partial y} \ \frac{\partial w}{\partial z} \ \left(\frac{\partial v}{\partial z} + \frac{\partial w}{\partial y}\right) \ \frac{\partial u}{\partial z} \ \frac{\partial u}{\partial y}\right\}. \tag{4}$$

Furthermore, the displacement field of eqns (1)–(3) should satisfy the equations of equilibrium and the traction-free conditions on the edges, $y = \pm b$ and top and bottom surfaces $z = \pm 2h$.

Spectral overlay finite element analysis

To study the free-edge effects in Pipes and Pagano's problem, two cross-ply laminates have been studied to demonstrate influence of free-edge effects. Each layer of the composite is assumed to be made of the same orthotropic material. The orientation of the axes differs from layer to layer. Referring to the principle direction of the material (x_1, x_2, x_3), the following engineering constants for the layers are used.

Typical high modulus graphite/epoxy:

$$E_{11} = 20.0 * 10^6 \text{ psi}; \qquad E_{22} = E_{33} = 2.1 * 10^6 \text{ psi}$$

$$G_{12} = G_{13} = G_{23} = 0.85 * 10^6 \text{ psi}; \qquad \nu_{12} = \nu_{13} = \nu_{23} = 0.21.$$

The interlaminar stress results presented here were obtained by using a spectral overlay finite element method. The material region under study in this work is reduced by symmetry conditions to that of one quadrant of the laminate cross-sectional region in the y–z plane as shown in Fig. 1 (shaded area). To represent the angle variation around the interface corner, a polar finite element mesh has been used near the free edge and rectangular mesh elsewhere (Fig. 2); a total of 168 finite elements have been used. Furthermore, two spectral overlays were put along the interface (Fig. 3) where high stress gradients occur. A detailed description of the spectral overlay finite element method can be found in Belytschko and Lu (1992).

The first example is the [0/90] laminate. Figures 4–9 show the stress distributions in the whole cross section. In this particular case, both σ_{zx} and σ_{xy}, as anticipated, vanish (Figs 9 and 7). This is because the applied strain coincides with the principle directions in both layers. σ_x is discontinuous across the interface, but it remains constant in each layer (Fig. 4). It is clearly seen Figs 5, 6 and 8 that the maxima of σ_y, σ_z and σ_{yz} are obtained at the corner of the interface and free edge. These maxima increase slightly with progressively more terms in the spectral approximation.

The distribution of σ_y along the free edge [Fig. 5(b)] suggests that a singularity exists at the interface corner. From Figs 5(b) and 8(b) we can also see that the σ_y and σ_{yz} do not satisfy the prescribed traction-free boundary condition at the same point, since the traction-free condition is a natural boundary condition. This and its high gradients are evidences of a stress singularity.

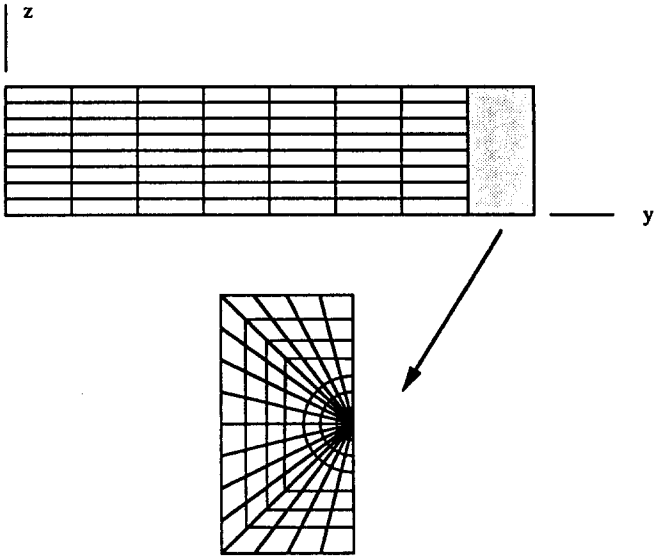

Fig. 2. Finite element mesh for composite laminates.

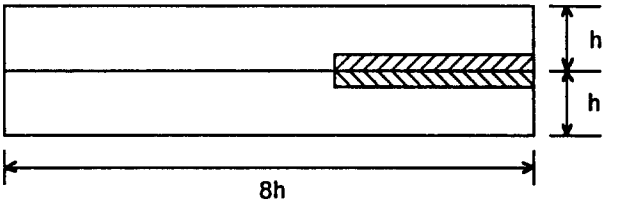

Fig. 3. Two spectral domains at interface.

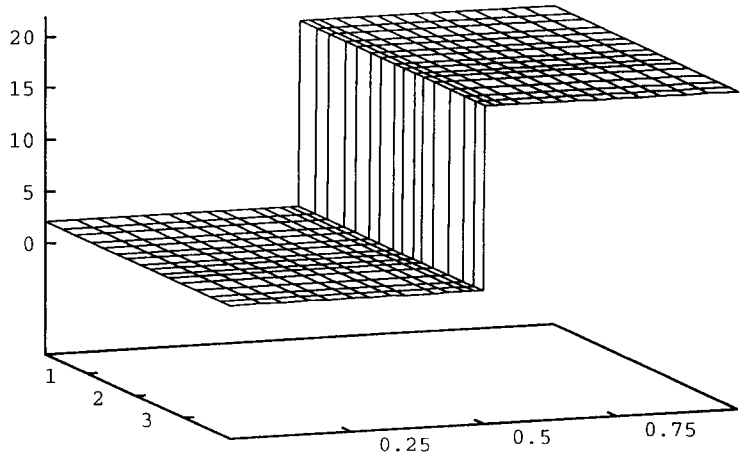

Fig. 4. The σ_x distributions for [0/90] laminate.

The second case is a [45/−45] angle-ply laminate. Some selected plots of the interlaminar stress distributions are given in Figs 10–12. As in the [0/90] laminate, a steep gradient occurs near the corner of the interface and the free edge, which indicates singular behavior at that point. The distribution of σ_{xy} is very complicated in this case (Fig. 11). It is discontinuous from layer to layer and the maximum is reached in both the lower and the upper layer near the corner of the interface and the free edge, but they have the opposite

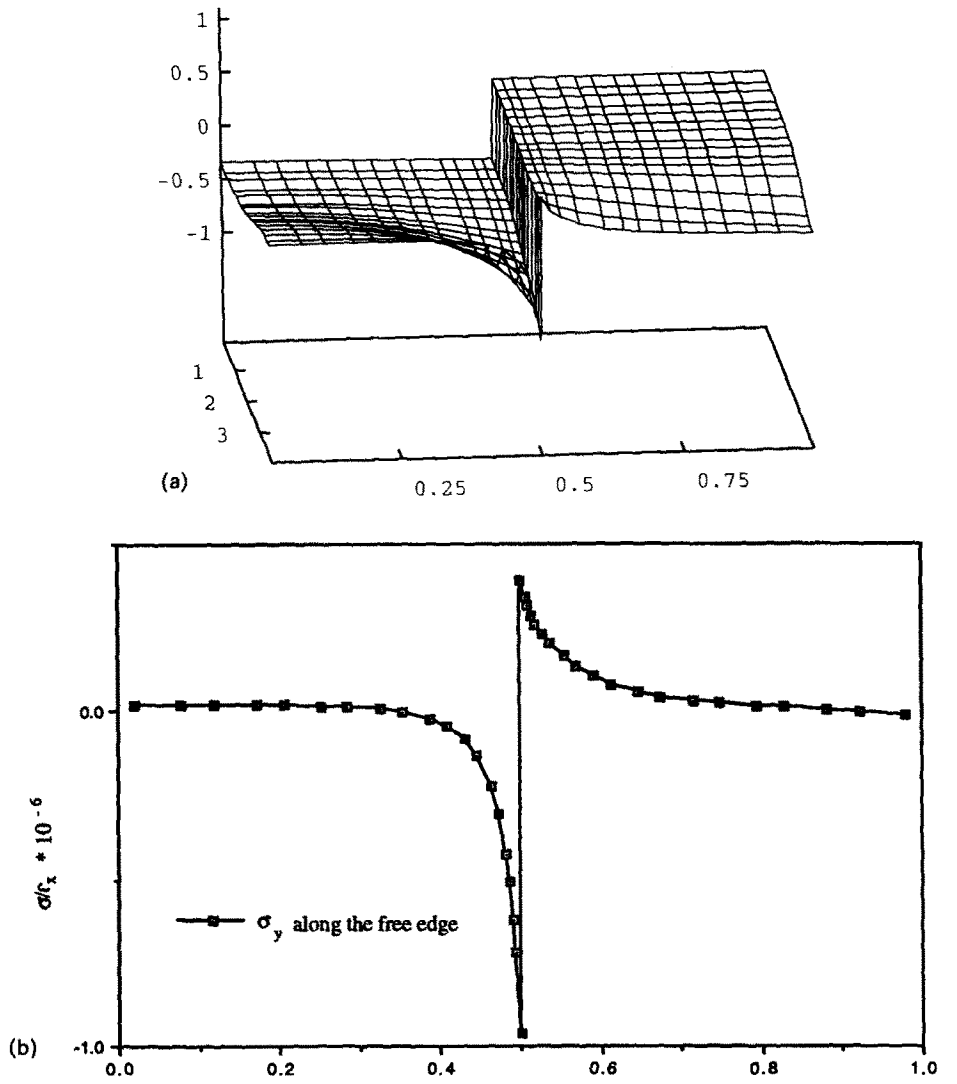

Fig. 5. (a) The σ_y distributions for [0/90] laminate; (b) σ_y along the free edge; [0/90] laminate.

signs. Along the free edge, σ_{xy} in the numerical solution shows significant errors in satisfying the traction-free condition near the interface.

The strength of the stress singularity in a composite laminate

For both laminates discussed above, the stress distribution indicates that a singularity exists at the corner of the interface and the free edge. For the present case, if one stress is singular at a point, then all the stresses are singular as well and singularities of all stresses should have the same strength. This is because all of these stresses are derivable from the equal-order derivatives of the same stress function, as shown by Lekhnitskii (1963).

To identify the stress singularities, the σ_{xy} stress was used in the least square fitting procedure by Raju and Crews (1981). Around the corner of the interface and the free edge, they assumed:

$$\sigma_{xy} = \alpha r^{\beta} + \gamma, \tag{5}$$

in above, α, β and γ can be determined by a least square technique. Raju and Crews demonstrated the stress singularity in the laminate composites and gave the singular order

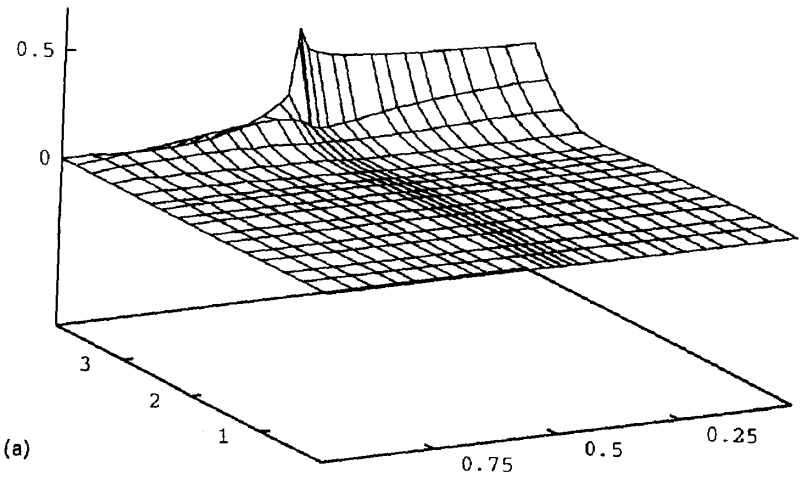

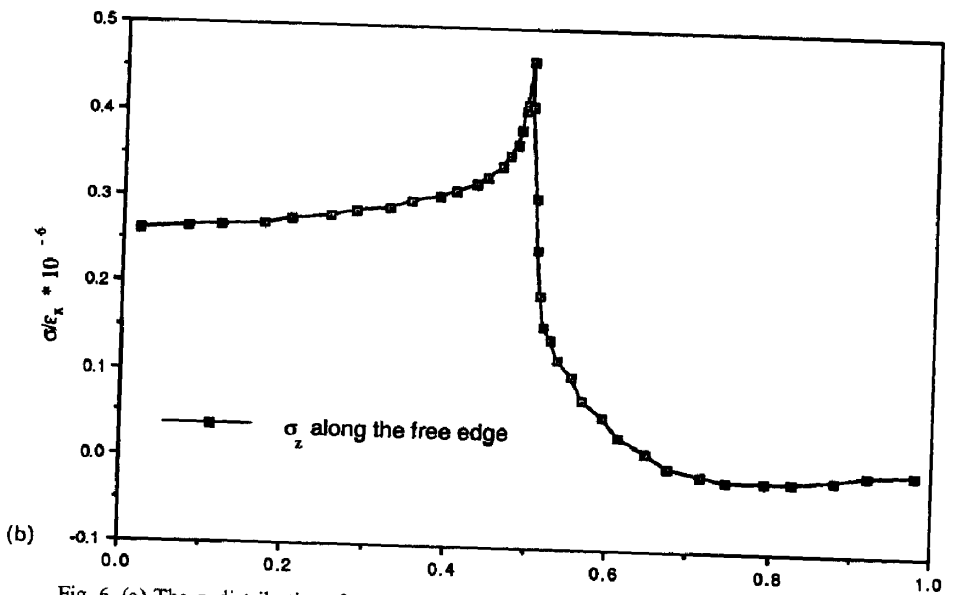

Fig. 6. (a) The σ_z distributions for [0/90] laminate; (b) σ_z along the free edge; [0/90] laminate.

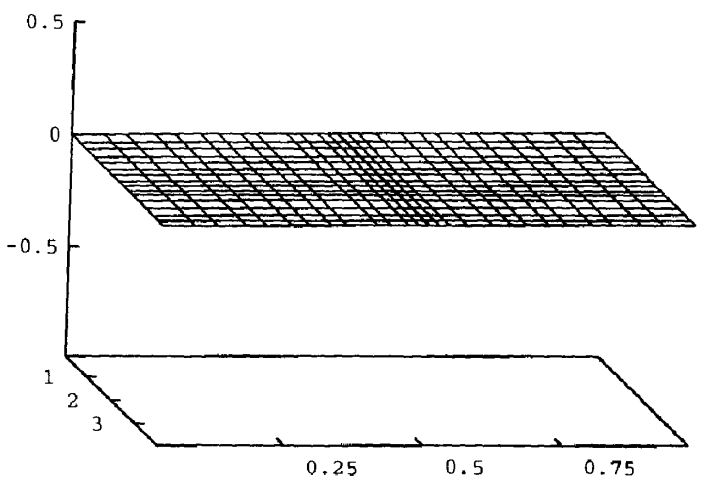

Fig. 7. The σ_{xy} distributions for [0/90] laminate.

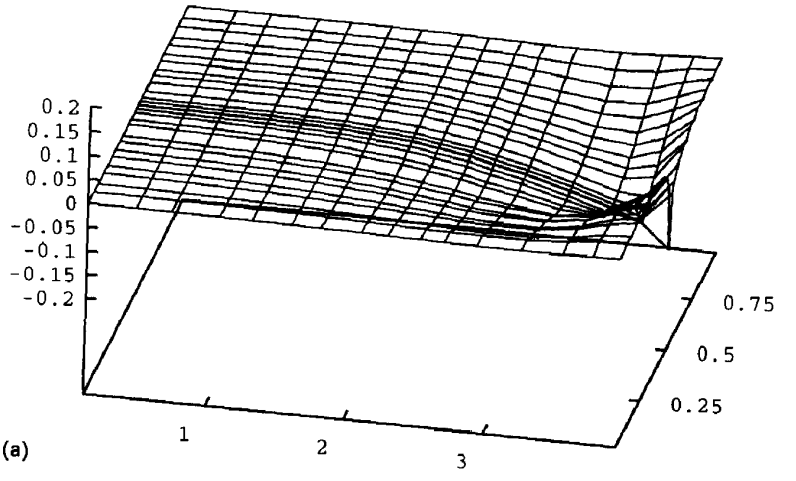

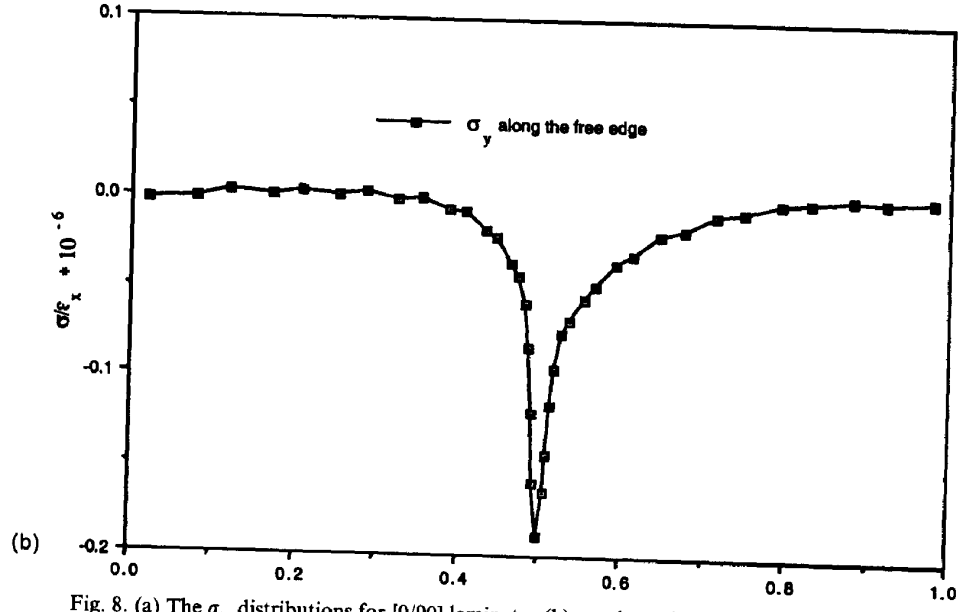

Fig. 8. (a) The σ_{yz} distributions for [0/90] laminate; (b) σ_{yz} along the free edge; [0/90] laminate.

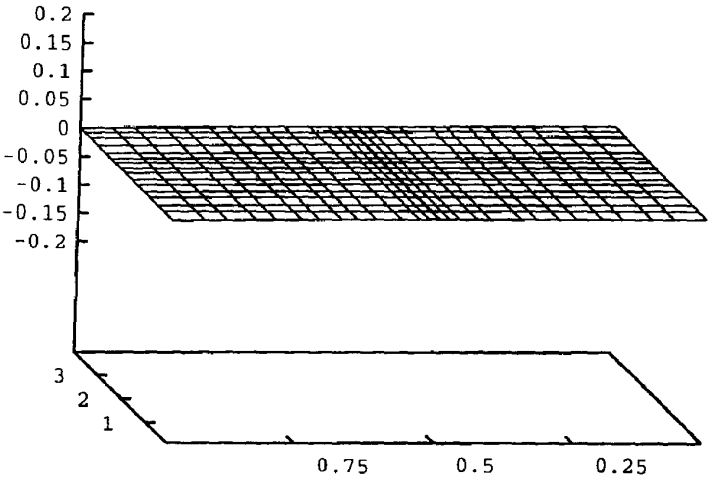

Fig. 9. The σ_{zx} distributions for [0/90] laminate.

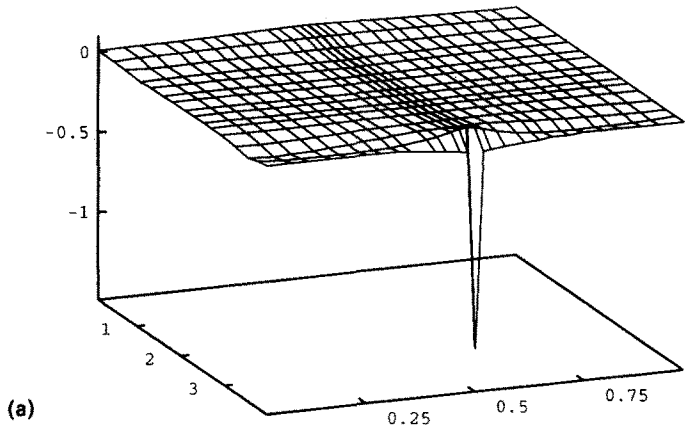

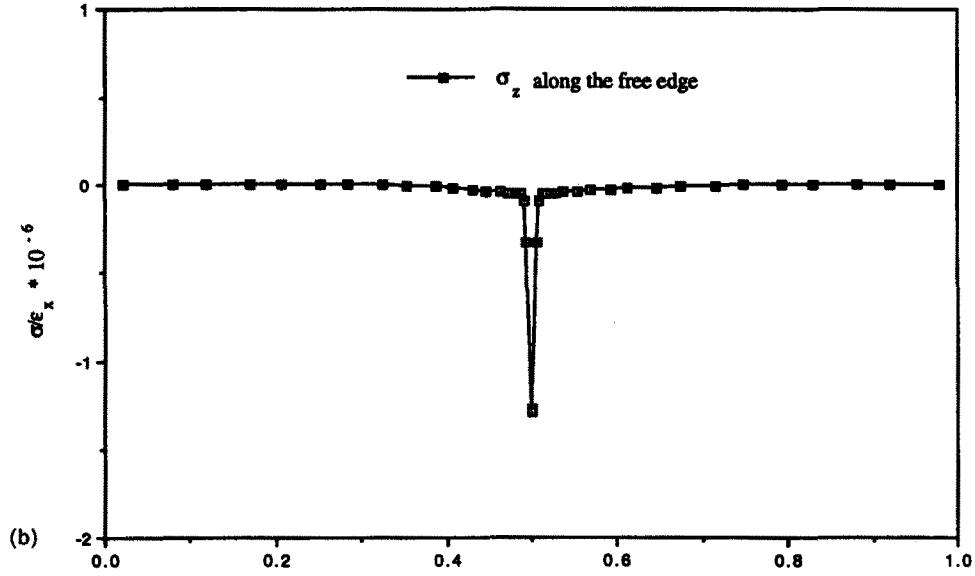

Fig. 10. (a) The σ_z distributions for [45/−45] laminate; (b) σ_z along the free edge; [45/−45] laminate.

from their finite element results for the first time, although the accuracy of their results may be questioned.

To obtain the strength of the stress singularity, we noticed that the singular stress behavior is localized in a very small zone, so each spectral domain was chosen to be quite small (0.1 h by 0.005 h; Fig. 3) and uses 30 terms in the direction normal to the free surface, and two terms in the other direction. Around the singular point, the stress distribution along the radial line from the singular point is assumed to take the form:

$$\sigma = Ar^{\alpha} + Br + C. \tag{6}$$

In the [±45] and [0/90] laminates, the values of the coefficients of eqn (6) obtained by least square method are given in Tables 1 and 2.

As expected, Table 1 shows that the singular order of σ_{xy} is almost the same as that of σ_{zz}. For the different laminates, the strengths of the stress singularity are in general different. Comparison with more exact results presented later in Table 6 and Fig. 22 show good agreement.

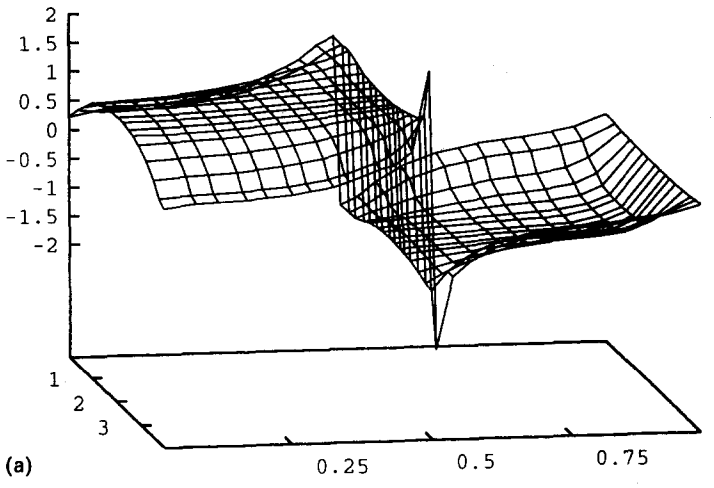

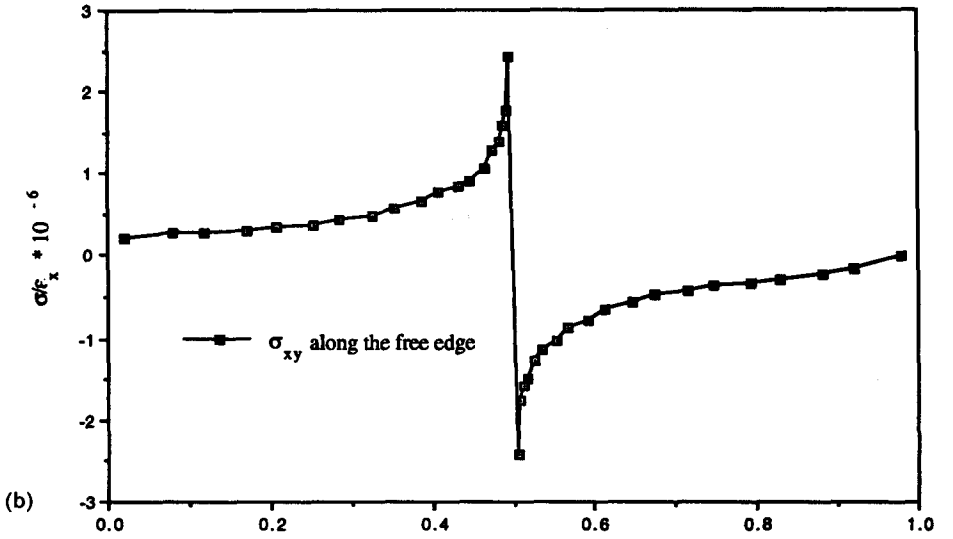

Fig. 11. (a) The σ_{xy} distributions for [45/−45] laminate; σ_{xy} along the free edge; [45/−45] laminate.

3. A FINITE ELEMENT APPROACH FOR DETERMINING THE STRENGTH OF THE STRESS SINGULARITY OF A WEDGE PROBLEM IN DISSIMILAR ISOTROPIC MATERIALS

Based on the Lekhnitskii's stress potentials and the theory of anisotropic elasticity, Wang and Choi (1982) determined the order of singularity of interlaminar stresses by solving the transcendental characteristic equation obtained from the homogeneous solutions for the problem. In the following sections of this paper, our attention will focus on constructing a new finite element scheme to determine the stress singularity in a two-material wedge. We first consider a two-isotropic-material wedge problem and then extend our method to a two-anisotropic-material wedge problem.

Formulation of the problem

Consider the geometry illustrated in Fig. 13. Two dissimilar half planes with Young's moduli E_1 and E_2 and Poisson's ratio ν_1 and ν_2 are joined together along $y = 0$ with a crack along $y = 0$, for $x \leqslant 0$. The boundary conditions are:

$$\sigma_\theta = \tau_{r\theta} = 0 \qquad \text{at } \theta = \pm\pi, \tag{7}$$

and the displacements u_r and u_θ and stresses σ_θ and $\tau_{r\theta}$ are continuous across the interface along $y = 0$ for $x \geqslant 0$.

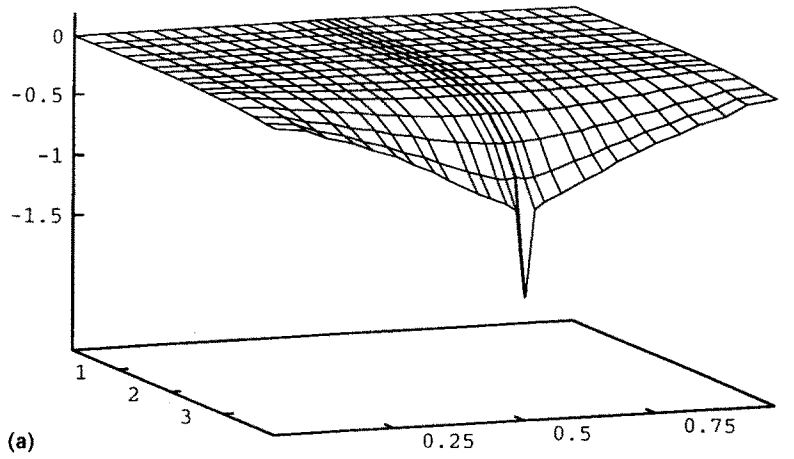

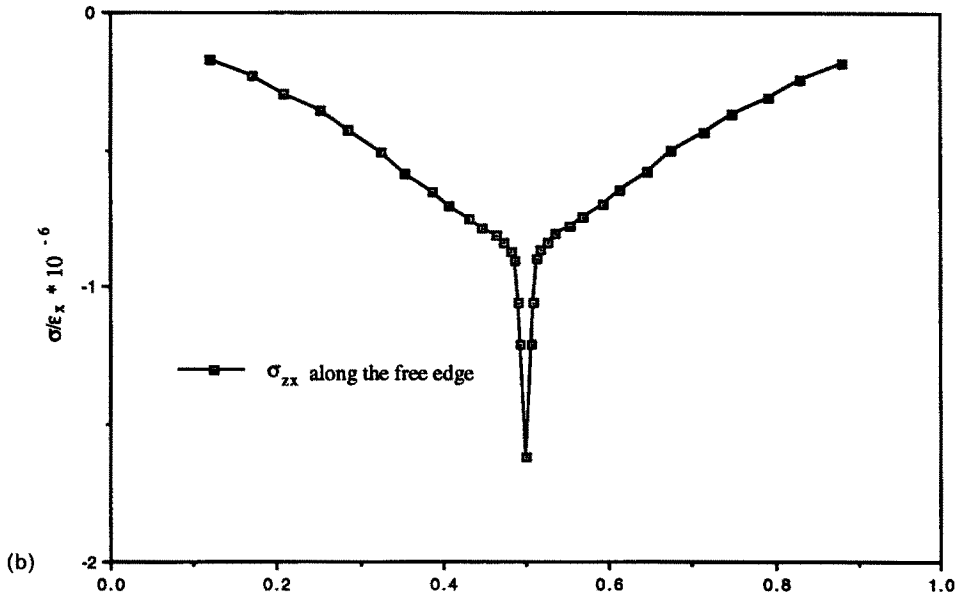

Fig. 12. (a) The σ_{zx} distributions for [45/−45] laminate; (b) σ_{xy} along the free edge; [45/−45] laminate.

The above homogeneous boundary conditions and interface continuity conditions can provide important information for determining the order of the stress singularity, which is the major concern in this paper. In the rest of this section, we will demonstrate how to employ an eigenfunction expansion technique to determine the order of the stress singularity by using a finite element method.

Method 1 : *a finite element method based on a stress function*

Basic formulation. Following the eigenfunction expansion procedure used by Williams (1957), Zak and Williams (1963), Barsoum (1988) and Swenson *et al.* (1990), the homogeneous solution of the above problem can be reduced to finding an Airy stress function $\chi(r, \theta)$, such that:

Table 1. The coefficients of eqn (6) in [±45] laminate

	α	A	B	C
σ_{xy}	−0.0272	2.47133	0.29563	−1.36064
σ_{zz}	−0.0277	−0.75125	−0.13023	−0.09301

Table 2. The coefficients of eqn (6) in [0/90] laminate

	α	A	B	C
σ_{yy}	−0.0308	−0.28177	−0.03649	−0.52411
σ_{zz}	−0.0306	0.38399	0.07680	−0.17463

$$\Delta^2\chi(r,\theta) = 0 \qquad \text{in } \Omega, \tag{8a}$$

$$\chi_{,rr} = 0 \qquad \theta = \pm\pi, \tag{8b}$$

$$-\frac{1}{r}\chi_{,r\theta} + \frac{1}{r^2}\chi_{,\theta} = 0 \qquad \theta = \pm\pi. \tag{8c}$$

We assume that the homogeneous solution for the Airy stress function can be expanded in terms of its eigenfunctions and each eigenfunction takes the separable form:

$$\chi(r,\theta,\lambda) = r^{\lambda+2}F(\theta), \tag{9}$$

where λ is an eigenvalue which in general is complex. For the crack problem shown in Fig. 13, separable stress functions of the same form are determined in each region, but it is required that the eigenvalues are equal: $\lambda_1 = \lambda_2$. This is done to assure continuity of displacement along the interface; subscripts 1 and 2 refer to the two materials.

Variational principle. To develop the finite element scheme for the determination of the stress singularity, we consider the homogeneous solution in a small neighborhood of the singular point; the polar coordinate (r, θ) is centered at the singular point as shown in Fig. 13. The potential energy can be written as:

$$\Pi = \int_\Omega \tfrac{1}{2}(\sigma_r\varepsilon_r + \sigma_\theta\varepsilon_\theta + \gamma_{r\theta}\tau_{r\theta})r\,\mathrm{d}r\,\mathrm{d}\theta - W^{EXT}. \tag{10}$$

The W^{EXT} can be omitted in the above because we are concerned only with the homogeneous solution. According to the principle of minimum potential energy, the static equilibrium state is determined by the variational equation:

$$\delta\Pi = \int_\Omega (\varepsilon_r\delta\sigma_r + \varepsilon_\theta\delta\sigma_\theta + \gamma_{r\theta}\delta\tau_{r\theta})r\,\mathrm{d}r\,\mathrm{d}\theta = 0, \tag{11}$$

or:

$$\delta\Pi = \int_\Omega (P_1\delta\chi_{,r} + P_2\delta\chi_{,rr} + P_3\delta\chi_{,r\theta} + P_4\delta\chi_{,\theta} + P_5\delta\chi_{,\theta\theta})\,\mathrm{d}r\,\mathrm{d}\theta = 0, \tag{12}$$

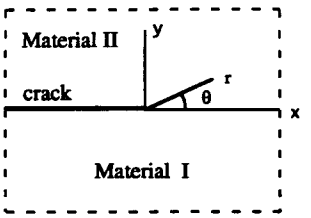

Fig. 13. The interface crack problem.

where

$$P_1 = \frac{1}{E_i}\left(\frac{1}{r}\chi_{,ir} + \frac{1}{r^2}\chi_{,\theta\theta} - \nu_i\chi_{,rr}\right), \tag{13}$$

$$P_2 = \frac{1}{E_i}\left[r\chi_{,rr} - \nu_i\left(\chi_{,r} + \frac{1}{r}\chi_{,\theta\theta}\right)\right], \tag{14}$$

$$P_3 = \frac{2(1+\nu_i)}{E_i}\left[\frac{1}{r}\chi_{,r\theta} - \frac{1}{r^2}\chi_{,\theta}\right], \tag{15}$$

$$P_4 = \frac{2(1+\nu_i)}{E_i}\left[\frac{1}{r^3}\chi_{,\theta} - \frac{1}{r^2}\chi_{,r\theta}\right], \tag{16}$$

$$P_5 = \frac{1}{rE_i}\left(\frac{1}{r}\chi_{,r} + \frac{1}{r^2}\chi_{,\theta\theta} - \nu_i\chi_{,rr}\right). \tag{17}$$

If we substitute eqn (9) directly into (12), the governing differential equation in the r direction cannot be satisfied, because the homogeneous boundary condition in the r direction has not been introduced and all terms depending on r will be canceled. Therefore, to determine the eigenvalue λ, it is necessary to integrate eqn (12) by parts with respect to r:

$$\delta\Pi = \int_\Omega ([P_{2,rr} - P_{1,r}]\delta_\chi + [P_4 - P_{3,r}]\delta\chi_{,\theta} + P_5\delta\chi_{,\theta\theta})\,\mathrm{d}r\,\mathrm{d}\theta + \text{Boundary terms in } r \text{ direction} = 0. \tag{18}$$

To determine the eigenfunctions, we omit all boundary terms. Substituting eqns (13)–(17) into eqn (18), we get:

$$\delta\Pi = \int_r r^{2\lambda+t}\,\mathrm{d}r\,\delta\Phi = 0, \tag{19}$$

or:

$$\delta\Phi = \int_\theta (Q_1\delta F(\theta) + Q_2\delta F'(\theta) + Q_3\delta F''(\theta))\,\mathrm{d}\theta = 0, \tag{20}$$

where

$$Q_1 = \frac{1}{E_i}\{(\lambda^4 + 4\lambda^3 + 4\lambda^2)F(\theta) - [\nu_i\lambda^2 + (1+\nu_i)\lambda]F''(\theta)\}, \tag{21}$$

$$Q_2 = -\frac{2}{E_i}(1+\nu_i)(\lambda^2 + 2\lambda + 1)F'(\theta) \tag{22}$$

$$Q_3 = \frac{1}{E_i}\{[-\nu_i\lambda^2 + (1-3\nu_i)\lambda + 2(1-\nu_i)]F(\theta) + F''(\theta)\}. \tag{23}$$

In eqn (20), to ensure boundedness of the strain energy it is necessary that:

$$Re\,\lambda \geqslant -1. \tag{24}$$

where $Re\,\lambda$ represents the real part of λ.

Finite element formulation. Since the weak form (20) involves derivatives of second order in the unknown function $F(\theta)$, a C^1 Hermitian interpolant must be used. The n unknowns of the problem are the nodal values F_i and their derivatives F_i'.

In the ith element, we assume:

$$F(\theta) = \sum_{a=1} (M_a(\theta)F_a + \bar{M}_a(\theta)F'_a), \tag{25}$$

where $M_a(\theta)$ are Hermite interpolants, so $M_a(\theta_b) = \delta_{ab}$, $M'_a(\theta_b) = 0$ and $\bar{M}_a(\theta_b) = 0$, $\bar{M}'_a(\theta_b) = \delta_{ab}$.

The above finite element interpolation leads to the following quartic eigenvalue equation:

$$(\lambda^4\mathbf{A} + \lambda^3\mathbf{B} + \lambda^2\mathbf{C} + \lambda\mathbf{D} + \mathbf{E})\mathbf{x} = 0, \tag{26}$$

where

$$A^e_{ab} = \frac{1}{E_i} N^e_a N^e_b, \tag{27}$$

$$B^e_{ab} = \frac{4}{E_i} N^e_a N^e_b, \tag{28}$$

$$C^e_{ab} = \frac{1}{E_i}(4N^e_a N^e_b - \nu_i N^e_a N^{e''}_b - 2(1+\nu_i)N^{e'}_a N^{e'}_b - \nu_i N^{e''}_a N^e_b), \tag{29}$$

$$D^e_{ab} = \frac{1}{E_i}[-(1+\nu_i)N^e_a N^{e''}_b - 4(1+\nu_i)N^{e'}_a N^{e'}_b + (1-3\nu_i)N^{e''}_a N^e_b], \tag{30}$$

$$E^e_{ab} = \frac{1}{E_i}[-2N^{e'}_a N^{e'}_b + (3-2\nu_i)N^{e''}_a N^e_b], \tag{31}$$

and

$$\mathbf{N}^e = \{M_1 \ \bar{M}_1 \ M_2 \ \bar{M}_2\}^e; \qquad \mathbf{x}^e = \{F_1 \ F'_1 \ F_2 \ F'_2\}^e. \tag{32}$$

This eigenvalue equation can be solved by converting it into the standard eigenvalue problem of size $4n$ by $4n$ (see Appendix).

Method 2: *A finite element method based on displacement*

Here we will give an alternative method based on the assumed separable form of the displacement field. Consider the same problem as shown in Fig. 13, the displacements in r and θ directions are denoted by $u(r, \theta)$ and $v(r, \theta)$, respectively. The strain energy of the body is given by eqn (10). The unknowns here are the displacements u and v.

We express the homogeneous solution of the displacements in the vicinity of the singular point in the separable form:

$$u(r, \theta) = r^{\lambda+1}F(\theta), \tag{33}$$

$$v(r, \theta) = r^{\lambda+1}G(\theta). \tag{34}$$

Substituting eqns (33)–(34) into (10), integrating it by parts with respect to r and omitting all boundary terms, gives:

$$\delta\Pi = \int_r r^{2\lambda+1}\, dr\, \delta\Phi = 0, \tag{35}$$

or:

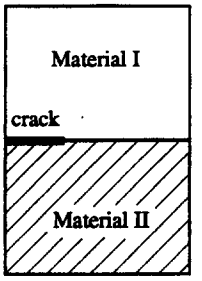

Fig. 14. A crack at a bimaterial interface.

$$\delta\Phi = \int_\theta (D_1\delta F(\theta) + D_2\delta F'(\theta) + E_1\delta G(\theta) + E_2\delta G'(\theta))\,\mathrm{d}\theta = 0, \tag{36}$$

where

$$D_1 = \frac{E_i}{1-\nu_i^2}[(-\lambda^2-1)F(\theta) + (1-\nu_i-\nu_i\lambda)G'(\theta)], \tag{37}$$

$$D_2 = \frac{E_i}{2(1+\nu_i)}[F'(\theta) + \lambda G(\theta)], \tag{38}$$

$$E_1 = -\frac{E_i}{2(1+\nu_i)}[(2+\lambda)F'(\theta) + (\lambda^2+2\lambda)G(\theta)], \tag{39}$$

$$E_2 = \frac{E_i}{1-\nu_i^2}[(\nu_i\lambda + 1 + \nu_i)F(\theta) + G'(\theta)]. \tag{40}$$

Using linear interpolants, eqn (36) leads to the following quadratic eigenvalue problem:

$$(\lambda^2\mathbf{A} + \lambda\mathbf{B} + \mathbf{C})\mathbf{x} = 0. \tag{41}$$

Employing a technique similar to that used for the quartic eigenvalue problem, we can convert eqn (41) to a standard eigenvalue problem of size $2n$ by $2n$.

Applications. The strength (β) of the crack-tip stress singularity (i.e. the radial dependence of each stress component $\sigma_{ij} = r^\beta f_{ij}(\theta)$) is directly related to the eigenvalue through $\beta = \lambda$.

Several cases were used to check the accuracy and correctness of the numerical method. These checks are performed by considering the interface crack problem shown in Fig. 14. When $E_1 = E_2$, and $\nu_1 = \nu_2$, the lowest eigenvalue is real and of order -0.4987 (method 1, 10 elements) or -0.4985 (method 2, 80 elements). This is in agreement with the well known results for the crack problem in the homogeneous material. When $E_1 \neq E_2$, and $\nu_1 \neq \nu_2$, Williams (1959), Rice and Sih (1965), England (1965) and others, using various analytical methods, arrived at the following expression for the singular order of the asymp-

Table 3. Order of stress singularity at the interfacial crack (plane stress condition)

E_1/E_2	λ (method 2)	λ (exact)
2.0	$-0.498480 + i0.037329$	$-0.5000 + i0.037306$
3.0	$-0.498478 + i0.056319$	$-0.5000 + i0.056283$
5.0	$-0.498473 + i0.075712$	$-0.5000 + i0.075666$
10.0	$-0.498468 + i0.093829$	$-0.5000 + i0.093774$
20.0	$-0.498465 + i0.104444$	$-0.5000 + i0.104386$
50.0	$-0.498462 + i0.111433$	$-0.5000 + i0.111372$
100.0	$-0.498461 + i0.113879$	$-0.5000 + i0.113817$

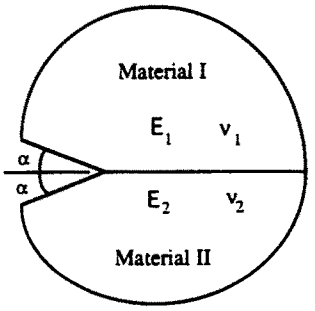

Fig. 15. The vertex of a bimaterial wedge.

totic field at the bi-material interface:

$$\lambda = -\tfrac{1}{2} + i\varepsilon, \tag{42}$$

where

$$\varepsilon = \frac{1}{2\pi} \ln \left[\frac{k_1/G_1 + 1/G_2}{k_2/G_2 + 1/G_1} \right]. \tag{43}$$

Subscripts 1 and 2 refer to the materials and $k = 3-4\nu$ for plane strain and $k = (3-\nu)/(1+\nu)$ for plane stress, G = shear modulus. The imaginary term ε leads to oscillations of the stresses as r approaches zero. The numerical results (method 2, 80 elements) summarized in Table 3 are in excellent agreement with the above analytical results.

Now considering the singular behavior at the vertex of a bi-material wedge (Fig. 15), we first let $E_1 = E_2$, and $\nu_1 = \nu_2 = 0.3$. When we open the wedge angle from a crack configuration ($\alpha = 0°$) to a half plane ($\alpha = 90°$), the eigenvalue changes from -0.4985 to 0 (Fig. 16). For $E_1/E_2 = \delta$, and $\nu_1 = \nu_2 = 0.3$, we list the eigenvalues in Table 4 for various values of α.

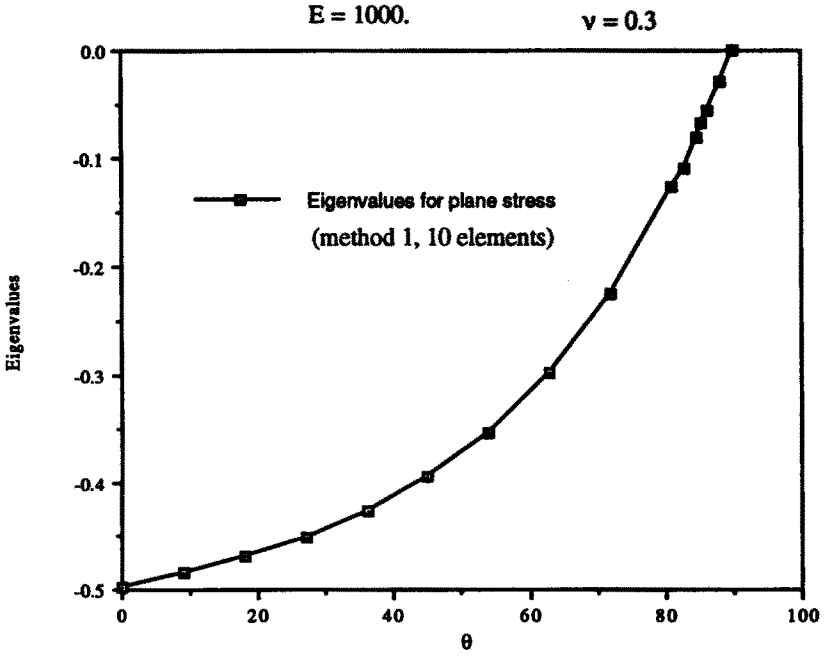

Fig. 16. Strength of stress singularity in homogeneous media.

Table 4. Eigenvalues of a two material wedge (plane stress condition; $\nu_1 = \nu_2 = 0.3$, $(E_1/E_2) = \delta$)

α (degrees)	λ (method 2, 80 elements) $\delta = 10$	$\delta = 50$	$\delta = 100$
0	$-0.49847 + i0.093829$	$-0.49846 + i0.11143$	$-0.49846 + i0.11388$
9	$-0.47173 + i0.097305$	$-0.47133 + i0.11519$	$-0.47162 + i0.11848$
18	$-0.44067 + i0.097601$	$-0.44026 + i0.11742$	$-0.43908 + i0.12014$
27	$-0.40429 + i0.092717$	$-0.40310 + i0.11391$	$-0.40292 + i0.11682$
36	$-0.36139 + i0.078461$	$-0.35855 + i0.10107$	$-0.35812 + i0.10412$
45	$-0.31053 + i0.038338$	$-0.30438 + i0.064857$	$-0.30343 + i0.068044$
54	-0.33072	-0.32296	-0.32186
63	-0.31687	-0.32185	-0.32253
72	-0.28964	-0.30369	-0.30558
81	-0.25197	-0.27424	-0.27722
90	-0.20350	-0.23332	-0.23734
99	-0.14238	-0.17880	-0.18370
108	-0.06501	-0.112647	-0.11212
117	0	-0.009402	-0.01553
119	0	0	0

In the case of $E_1 = 1$, $E_2 = 100$, and $\nu_1 = \nu_2 = 0.3$, the numerical eigenvalues for various values of α are shown in Fig. 17 (plane stress condition). These results indicate three distinct regions.

In the first region, the eigenvalues are complex, which gives a singular and oscillatory behavior to the stresses. In this region, the absolute value of the real parts of the eigenvalue decreases from 0.4985 ($\alpha = 0°$) to 0.274 ($\alpha = 49°$), while the imaginary part of the eigenvalue increases slightly as α varies from 0° to 22° and decreases to 0 at $\alpha = 49°$. In the second region, the stresses remain singular but there are no oscillations. The interesting point is that the strength of the singularity increases a little from 0.274 to 0.315 as α varies from 49° to 52° and then decreases to 0 ($\alpha = 119°$). Finally, there is a region with no singular stress ($\alpha > 119°$).

The last example is the free edge problem at the bimaterial interface (Fig. 18). When

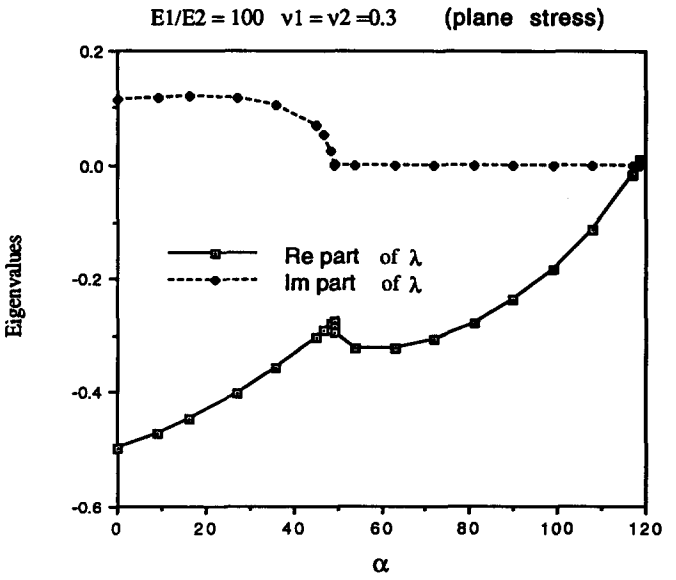

Fig. 17. Eigenvalues at the tip of interface crack (method 2, 80 elements); α given in degrees.

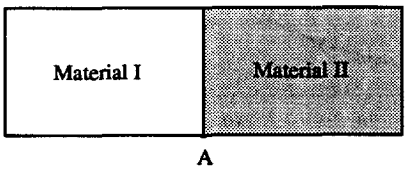

Fig. 18. The free-edge problem for a bimaterial interface.

Table 5. Eigenvalues at bimaterial free edge (method 1, 10 elements)

E_1/E_2	2	5	10	20	50	100	200	5000
λ_a†	−0.09185	−0.17059	−0.20350	−0.22173	−0.23334	−0.23734	−0.23936	−0.24132
λ_b‡	−0.10653	−0.20111	−0.24148	−0.26406	−0.27851	−0.28549	−0.28602	−0.28853

† plane stress
‡ plain strain.

the two materials are different, a stress singularity occurs at point A. In the case of a nearly rigid bottom plate ($E_2/E_1 = 5000$, $\nu_1 = \nu_2 = 0.3$), λ has the value of -0.2885, which agrees with the -0.289 obtained by Williams (1952) and Hein and Erdogan (1971) who assumed $E_2/E_1 =$ infinite, and $\nu_1 = \nu_2 = 0.3$. The numerical results (method, 1, 10 elements) are illustrated in Table 5 and Fig. 19.

4. A FINITE ELEMENT METHOD FOR ANISOTROPIC MATERIALS

Basic formulation

We consider Pipes and Pagano's problem (Section 2, Fig. 1). In the present study, we wish to investigate the stress singularities in the region near the junction of the free edge and the interface. We consider the asymptotic displacement field in a small neighborhood of the singular point at the origin, and assume that the complementary displacement field of the asymptotic solution near the singular point can be expressed as:

$$u_x = u_x(r, \theta), \tag{44}$$

$$u_r = u_r(r, \theta), \tag{45}$$

$$u_\theta = u_\theta(r, \theta). \tag{46}$$

To expedite further developments, we transform the displacement components from polar coordinates to Cartesian coordinates. Thus, we have:

$$u_x = u_x; \quad u_y = u_r \cos\theta - u_\theta \sin\theta; \quad u_z = u_r \sin\theta + u_\theta \cos\theta. \tag{47}$$

It should be noted that the stress components associated with the homogeneous

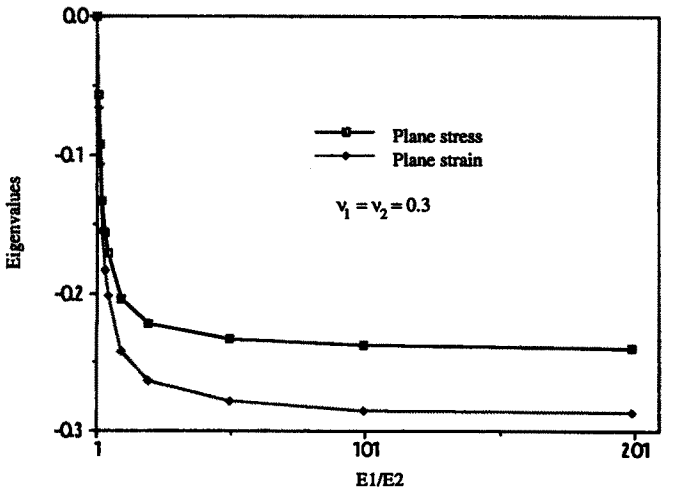

Fig. 19. Strength of stress singularity at A (method 1, 10 elements).

displacement field are independent of the axial coordinate x, and for the homogeneous solution of the asymptotic field, the boundary conditions are homogeneous.

Weak formulation

Let Π denote the strain energy in the body, which is given by:

$$\Pi = \int_\Omega \tfrac{1}{2}\boldsymbol{\varepsilon}^T\boldsymbol{\sigma} r \, \mathrm{d}r \, \mathrm{d}\theta = \int_\Omega \tfrac{1}{2}\boldsymbol{\varepsilon}^T\mathbf{C}\boldsymbol{\varepsilon} r \, \mathrm{d}r \, \mathrm{d}\theta. \tag{48}$$

Where ($\varepsilon_x = 0$):

$$\boldsymbol{\varepsilon}^T = \{\varepsilon_y \;\; \varepsilon_z \;\; \gamma_{yz} \;\; \gamma_{zx} \;\; \gamma_{xy}\}, \tag{49}$$

$$\boldsymbol{\sigma}^T = \{\sigma_y \;\; \sigma_z \;\; \tau_{yz} \;\; \tau_{zx}\tau_{xy}\} = (C_\varepsilon)^T, \tag{50}$$

and

$$\mathbf{C} = \begin{bmatrix} C_{22} & C_{23} & 0 & 0 & C_{26} \\ C_{32} & C_{33} & 0 & 0 & C_{36} \\ 0 & 0 & C_{44} & C_{45} & 0 \\ 0 & 0 & C_{54} & C_{55} & 0 \\ C_{62} & C_{63} & 0 & 0 & C_{66} \end{bmatrix}. \tag{51}$$

The displacement field corresponding to the equilibrium configuration is determined by:

$$\delta\Pi = \int_\Omega \boldsymbol{\sigma}\delta\boldsymbol{\varepsilon}^T r \, \mathrm{d}r \, \mathrm{d}\theta = 0, \tag{52}$$

or:

$$\delta\Pi = \int_\Omega \delta\mathbf{u}^T \left\{\mathbf{S}_0\boldsymbol{\sigma} + r\mathbf{S}_1\frac{\partial\boldsymbol{\sigma}}{\partial r}\right\} \mathrm{d}r \, \partial\theta = 0, \tag{53}$$

where $\boldsymbol{\sigma}$ is given by eqn (50) and,

$$\delta\mathbf{u}^T = \{\delta u_r \;\; \delta u_{r,\theta} \;\; \delta u_\theta \;\; \delta u_{\theta,\theta} \;\; \delta u_x \;\; \delta u_{x,\theta}\} \tag{54}$$

$$S_0 = \begin{bmatrix} s^2-c^2 & c^2-s^2 & -4sc & 0 & 0 \\ -sc & sc & c^2-s^2 & 0 & 0 \\ 2sc & -2sc & -2(c^2-s^2) & 0 & 0 \\ s^2 & c^2 & -2sc & 0 & 0 \\ 0 & 0 & 0 & -s & -c \\ 0 & 0 & 0 & c & -s \end{bmatrix}, \tag{55}$$

$$S_1 = \begin{bmatrix} c^2 & s^2 & 2sc & 0 & 0 \\ 0 & 0 & 0 & 0 & 0 \\ -sc & sc & c^2-s^2 & 0 & 0 \\ 0 & 0 & 0 & 0 & 0 \\ 0 & 0 & 0 & s & c \\ 0 & 0 & 0 & 0 & 0 \end{bmatrix}, \tag{56}$$

in the above, $s = \sin\theta$ and $c = \cos\theta$.

Assume that the displacement field [eqns (44)–(46)] takes the separable form:

$$u_x = r^{\lambda+1}F_3(\theta); \quad u_r = r^{\lambda+1}F_1(\theta); \quad u_\theta = r^{\lambda+1}F_2(\theta). \tag{57}$$

Equations (57) are required to satisfy the homogeneous boundary conditions and interface continuity conditions. This leads to an eigenvalue problem for determining the values of λ. It is noted that the value of λ is required to satisfy the condition:

$$Re\,\lambda \geqslant -1, \tag{58}$$

to ensure the displacement is finite at the origin point.

Substituting (57) into (49), gives:

$$\boldsymbol{\varepsilon} = r^{\lambda}(\lambda\mathbf{E}_0 + \mathbf{E}_1)\mathbf{d}, \tag{59}$$

where:

$$\mathbf{d} = \{F_1(\theta)\ F_1'(\theta)\ F_2(\theta)\ F_2'(\theta)\ F_3(\theta)\ F_3'(\theta)\}^T, \tag{60}$$

$$\mathbf{E}_0 = \mathbf{S}_1^T, \tag{61}$$

$$\mathbf{E}_1 = \begin{bmatrix} 1 & -sc & 0 & s^2 & 0 & 0 \\ 1 & sc & 0 & c^2 & 0 & 0 \\ 0 & c^2-s^2 & 0 & -2c & 0 & 0 \\ 0 & 0 & 0 & 0 & s & c \\ 0 & 0 & 0 & 0 & c & -s \end{bmatrix}. \tag{62}$$

The stresses are given by:

$$\boldsymbol{\sigma} = r^{\lambda}(\lambda\mathbf{T}_0 + \mathbf{T}_1)\mathbf{d}, \tag{63}$$

where

$$\mathbf{T}_0 = \mathbf{C}\mathbf{E}_0; \quad \mathbf{T}_1 = \mathbf{C}\mathbf{E}_1. \tag{64}$$

Substituting (63) into (53), and noticing $\delta\mathbf{u}^T = r^{\lambda+1}\delta\mathbf{d}^T$, we get:

$$\delta\Phi = \int_\theta \delta\mathbf{d}^T[\lambda^2\mathbf{S}_1\mathbf{T}_0 + \lambda(\mathbf{S}_0\mathbf{T}_0 + \mathbf{S}_1\mathbf{T}_1) + \mathbf{S}_0\mathbf{T}_1]\delta\mathbf{d}\,d\theta = 0. \tag{65}$$

Finite element formulation

The weak form (65) may now be used as a basis for formulating a finite element approximation. To this end let $-(\pi/2) = \theta_0 < \theta_1 < \cdots < \theta_{n+1} = (\pi/2)$ be a partition of the

interval $(-(\pi/2),(\pi/2))$ into subintervals $\Omega_1 = (\theta^i_1, \theta^i_2)$ of the length h^e. The unknown functions $F_i(\theta)$ are approximated by shape functions N_I and nodal values F_{iI}

$$F_i(\theta) = F_{iI} N_I(\theta). \tag{66}$$

The discrete form of the gradient operator can be expressed as:

$$F'_i(\theta) = F_{iI} N'_I(\theta). \tag{67}$$

Substituting (66)–(67) into (65) yields:

$$\sum_{e=1}^{nelem} \int_{\theta_e} \delta \mathbf{x}_e^T \mathbf{N}_e^T [\lambda^2 \mathbf{S}_1 \mathbf{T}_0 + \lambda(\mathbf{S}_0 \mathbf{T}_0 + \mathbf{S}_1 \mathbf{T}_1) + \mathbf{S}_0 \mathbf{T}_1] \mathbf{N}_e \delta \mathbf{x}_e \, d\theta = 0, \tag{68}$$

where

$$\mathbf{x}_e^T = \{F_{11} \;\; F_{12} \;\; F_{21} \;\; F_{22} \;\; F_{31} \;\; F_{32}\}. \tag{69}$$

Equation (68) can be rewritten as:

$$(\lambda^2 \mathbf{A} + \lambda \mathbf{B} + \mathbf{D})\mathbf{x} = \mathbf{0}, \tag{70}$$

where in each element:

$$\mathbf{A}_e = \int_{\theta_e} \mathbf{N}_e^T \mathbf{S}_1 \mathbf{T}_0 \mathbf{N}_e \, d\theta, \tag{71}$$

$$\mathbf{B}_e = \int_{\theta_e} \mathbf{N}_e^T (\mathbf{S}_0 \mathbf{T}_0 + \mathbf{S}_1 \mathbf{T}_1) \mathbf{N}_e \, d\theta, \tag{72}$$

$$\mathbf{D}_e = \int_{\theta_e} \mathbf{N}_e^T \mathbf{S}_0 \mathbf{T}_1 \mathbf{N}_e \, d\theta. \tag{73}$$

Numerical results

We proceed to investigate two general cases:

(i) free edge effects in the laminate;
(ii) the interlaminar crack between dissimilar anisotropic laminates in a composite.

Two different composite materials are used for the numerical calculations.

Composite A is a typical high modulus graphite/epoxy; the material constants were given in Section 2.

Composite B: (T300/5208 graphite/epoxy)

$$E_1 = E_2 = 1.54 \cdot 10^6 \text{ psi}; \quad E_3 = 22 \cdot 10^6 \text{ psi};$$

$$G_{21} = G_{23} = G_{31} = 0.81 \cdot 10^6 \text{ psi}; \quad \nu_{21} = \nu_{31} = \nu_{32} = 0.28.$$

In the above, E_i are the Young's moduli, G_{ij} the shear moduli, and ν_{ij} the Poisson's ratios. The **C** matrix [see eqn (51)] is obtained by using the relations derived by Pipes and Pagano (1970).

Free edge problem

For the commonly used $[\pm\alpha]$ angle-ply composite (Fig. 1), the order of the stress singularity is a function of the fiber orientation α. Finite element results of λ_1 for each of

Table 6. Eigenvalues for free-edge stresses associated with $[\pm\alpha]$ fiber orientation composites (40 elements)

$\pm\alpha$	15	30	45	60	75
λ_1 (Comp. A)	−0.001994	−0.011592	−0.025403	−0.020183	−0.003830
λ_1 (Comp. B)	−0.002574	−0.022339	−0.033142	−0.029928	−0.005127

the $[\pm\alpha]$ fiber composites are summarized in Table 6 and shown in Fig. 20 and Fig. 21. In the case of composite A, the strongest stress singularity, which is equal to −0.027334, occurs in a composite laminate having [±53 degree] fiber orientation. For the [±45] composite, the strength of stress singularity is −0.025403, which agrees with the value of −0.0274 obtained by spectral overlay finite element method and −0.02557 by Wang and Choi (1982).

In the case of free-edge stress associated with the [90 degree/α] fiber orientation in composite A, Fig. 22 shows that the strength of the stress singularity at point A is not equal to that at point B because the configuration is not symmetric about z axis.

Interlaminar crack problems

The finite element approach presented in this section can be easily extended to the interlaminar crack problem between dissimilar anisotropic materials.

In the previous section we have shown that the dominant term in the interface crack between two isotropic materials is related to the two complex and conjugate eigenvalues λ_1 and λ_2 with real parts equal to −0.5. In the case of an interlaminar crack between angle-ply composites, things become more complicated. The strength of the stress singularity is related to the first three eigenvalues λ_1, λ_2 and λ_3, where λ_1 is a real number. The numerical results (Tables 7 and 8) show λ_1 close to −0.5, and λ_2 and λ_3 are complex and conjugate

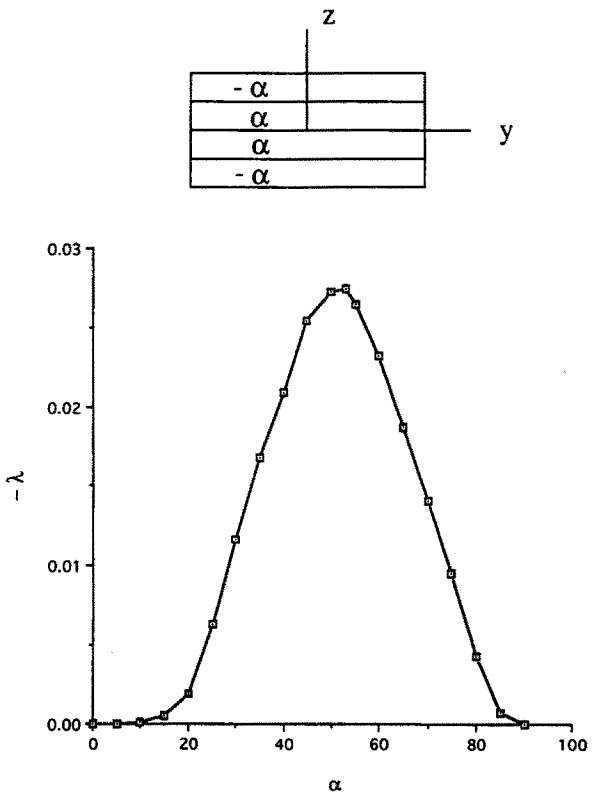

Fig. 20. Strength of stress singularity in $[\alpha/-\alpha]$ graphite-epoxy composites (40 elements).

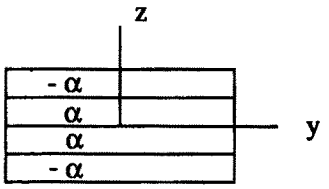

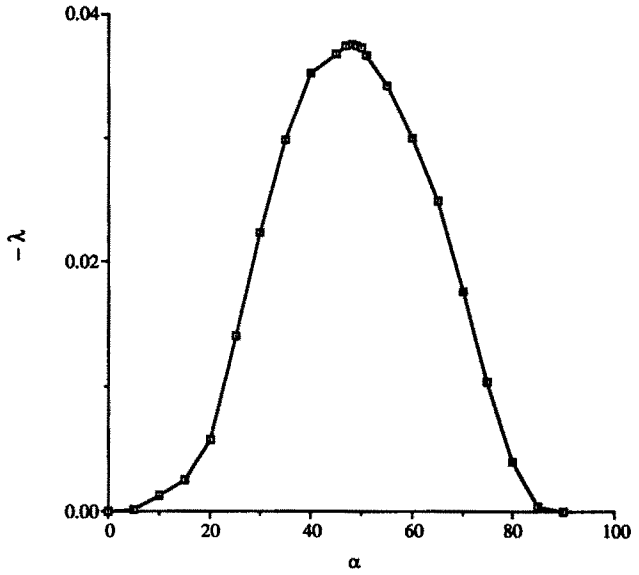

Fig. 21. Strength of stress singularity in $[\alpha/-\alpha]$ T300/5208 graphite/epoxy (40 elements).

eigenvalues. The imaginary parts of λ_2 and λ_3 are very small in general, and decrease as α changes in either direction. In the limited cases $\alpha = 0$ and $\alpha = \pi/2$, the imaginary parts of λ_2 and λ_3 vanish since the two materials become identical with a single phase.

4. CONCLUSION

At the present time, experimental agreement has not been established between the strength of the singularity and failure. However, effective methods for determining the strength of the singularity are clearly needed. In this paper, two finite element methods for determining the strength of the singularity have been presented for the interface in both isotropic and anisotropic materials. The methods are based on an eigenfunction expansion method and involve the solutions of quadratic eigenvalue problems. The results agree very

Table 7. The first three eigenvalues for interlaminar crack problems associated with $[\pm\alpha]$ graphite-epoxy composites (40 elements)

α	λ_1	λ_2 and λ_3
15	−0.502955	$-0.504541 \pm i0.004912$
30	−0.503223	$-0.505145 \pm i0.023907$
45	−0.503605	$-0.507170 \pm i0.034032$
60	−0.503867	$-0.509929 \pm i0.028159$
75	−0.503669	$-0.511536 \pm i0.013336$

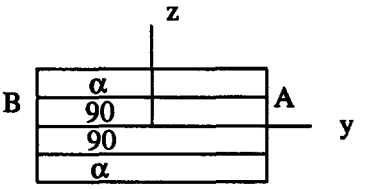

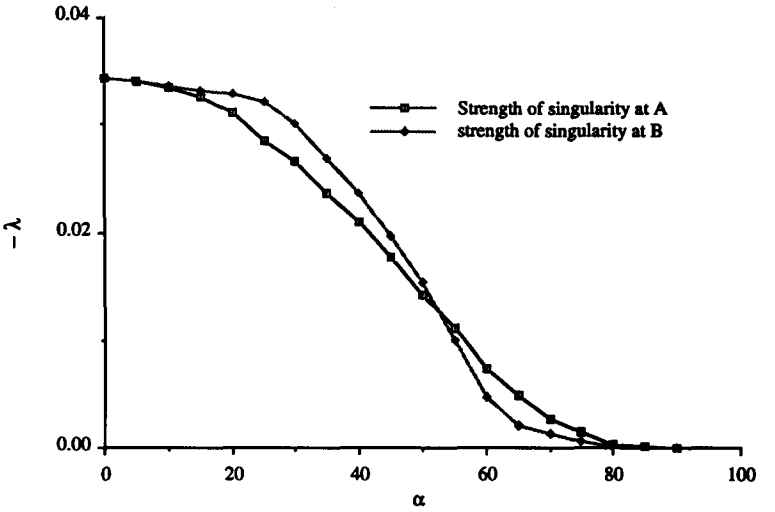

Fig. 22. Strength of stress singularity in [α/90] graphite/epoxy composites (40 elements).

well with previous solutions and some new solutions are given. In addition, it has been shown that if a method with high resolution, such as the spectral overlay is used, good estimates of the strength of the singularity can be obtained by a least-square fit.

In the case of an interface at a free edge, the singularity is quite weak with an exponent of order 0.03. The new results obtained here show that the strength of the singularity decreases monotonically in a [α/90°] interface as α tends to 90°; at 45° the strength is half of that at zero. In [−α/α] plies, the strength is maximum near 45° and is approximately parabolic, with values of less than 0.01 for $\alpha < 25°$.

The eigenvalue methods correctly reproduce that for an interface crack the eigenvalues are complex, indicating oscillatory stresses. New results are obtained for an interlaminar crack between [−α/α] composites. The results show that the real part of the singularity is almost exactly −0.5 (within 1%).

Table 8. The first three eigenvalues for interlaminar crack problems associated with [±α] T300/5208 graphite-epoxy composites (40 elements)

α	λ_1	λ_2 and λ_3
15	−0.502974	$-0.504635 \pm i0.008496$
30	−0.503262	$-0.505572 \pm i0.027292$
45	−0.503806	$-0.508176 \pm i0.034121$
60	−0.504283	$-0.511358 \pm i0.025442$
75	−0.503799	$-0.513247 \pm i0.064810$

Whereas standard finite element and finite difference methods give ambiguous stress results at the interfaces of the composite laminates because of the presence of weak stress singularities, the spectral overlay can provide solutions that agree closely with the eigenvalue methods. However, in order to achieve these solutions, considerable resolution must be introduced in a small area near the free edge and interface.

While the eigenvalue methods cannot be used to ascertain the coefficient of the singular terms, once the strength of the singularity is known, these singular terms can be included in the pertinent elements to obtain a complete solution. This, however, is quite involved and the results obtained by the spectral overlay show that both the coefficient and the strength of the singularity can effectively be obtained by this method.

Acknowledgement—The support of NASA Langley to Northwestern University is gratefully acknowledged.

REFERENCES

Barsoum, R. S. (1988). Applications of the finite element iterative method to the eigenvalue problem of crack between dissimilar media. *Int. J. Numer. Meth. Engng* **26,** 541–554.

Barsoum, R. S. (1990). Asymptotic fields at interfaces using the finite element iterative method. *Comput. Struct.* **35,** 285–292.

Bazant, Z. P. and Estenssord, L. F. (1979). Surface singularity and crack progagation. *Int. J. Solids Structures* **15,** 405–426.

Belytschko, T., Fish, J. and Bayliss, A. (1990). The spectral overlay on finite elements for problems with high gradients. *Comput. Meth. Appl. Mech. Engng* **81,** 71–89.

Belytschko, T. and Lu, Y. Y. (1992). A curvilinear spectral overlay methods for high gradient problems. *Comput. Meth. Appl. Mech. Engng* **95,** 383–396.

Clements, D. L. (1971). A crack between dissimilar anisotropic media. *Int. J. Engng Sci.* **9,** 257–265.

Comninou, M. (1977). The interface crack. *J. Appl. Mech.* **44,** 19–27.

Dundurs, J. (1969). Discussion. *J. Appl. Mech.* **36,** 650–652.

England, A. H. (1965). A crack between dissimilar media. *J. Appl. Mech.* **32,** 400–402.

Erdogan, F. (1965). Stress distribution in bonded dissimilar materials with cracks. *J. Appl. Mech.* **32,** 400–402.

Goton, M. (1967). Some problems of bonded anisotropic planes with cracks along the bond. *Int. J. Fracture Mech.* **3,** 253–265.

Gu, Q. and Reddy, J. N. (1992). Non-linear analysis of free-edge effects in composite laminates subjected to axial loads. *Int. J. Non-Linear Mech.* **27,** 27–41.

Hein, V. L. and Erdogan, F. (1971). Stresses singularities in a two-material wedge. *Int. J. Fracture Mech.* **7,** 317–330.

Herakovich, C. T., Nagarkar, A. and O'Brien, D. A. (1979). Failure analysis of composite laminates with free edges. *Modern Development in Composite Materials and Structures* (Edited by J. R. Vinson), 53–66.

Hsiao, T. L. (1991). A global-local finite element for general composite structure. *Comput. Struct.* **40,** 719–730.

Hsu, P. W. and Herakovich, C. T. (1977). Edge effects in angle-ply composite laminates. *J. Compos. Mater.* **11,** 422–428.

Lekhnitskii, S. G. (1963). *Theory of Elasticity of Anisotropic Body*. Holden-Day, Inc., San Francisco.

Pipes, R. B. and Pagano, N. J. (1970). Interlaminar stresses in composite laminates under uniform axial extension. *J. Compos. Mater.* **4,** 538–548.

Raju, I. S. and Crews, J. H. Jr (1981). Interlaminar stress singularities at a straight free edge in composite laminates. *Comput. Struct.* **4,** 21–28.

Rice, J. R. and Sih, G. C. (1965). Plane problems of cracks in dissimilar media. *J. Appl. Mech.* **32,** 418–423.

Somaratna, N. and Ting, T. C. T. (1986). Three-dimensional stress singularities in anisotropic materials and composites. *Int. J. Engng Sci.* **24,** 1115–1134.

Spilker, R. I. and Chou, S. C. (1980). Edge effects in symmetric composite laminates: importance of satisfying the traction-free-degree conditions. *J. Compos. Mater.* **14,** 2–20.

Swenson, M., Ortiz, M. and Shih, C. F. (1990). A finite element method for determining the angular variation of asymptotic crack tip fields. *Int. J. Fracture* **45,** 51–64.

Tang, S. and Levy, A. (1975). A boundary layer theory—part II: extension of laminated finite strip. *J. Compos. Mater.* **9,** 42–52.

Wang, S. S. and Choi, I. (1982). The interface crack between dissimilar anisotropic composite materials. *J. Appl. Mech.* **49,** 541–548.

Wang, S. S. and Choi, I. (1983). Boundary-layer effects in composite laminates—part 1: free edge stress singularities. *J. Appl. Mech.* **50,** 169–178.

Wang, A. S. D. and Crossman, F. W. (1977). Some new results on edge effects in symmetric composite laminates. *J. Compos. Mater.* **11,** 92–106.

Wang, J. T. S. and Dickson, J. N. (1978). Interlaminar stresses in symmetric composite laminates. *J. Compos. Mater.* **12,** 390–402.

Whitecomb, J. D., Raju, J. S. and Goree, J. G. (1982). Reliability of the finite element method for calculating free edge stresses in composite laminates. *Comput. Struct.* **15,** 23–37.

Williams, M. L. (1952). Stress singularities resulting from various boundary conditions in angular corners of plates in extension. *J. Appl. Mech.* **19,** 526–528.

Williams, M. L. (1957). On the stress distribution at the base of a stationary crack. *J. Appl. Mech.* **24,** 109.

Williams, M. L. (1959). The stress around a fault or crack in dissimilar media. *Bull. Seismol. Soc. Am.* **49,** 199–204.
Willis, J. R. (1971). Fracture mechanics of interface cracks. *J. Mech. Phys. Solid.* **19,** 253–268.
Ye, L. (1990). Some characteristics of distributions of free-edge interlaminar stresses in composite laminates. *Int. J. Solids Structures* **26,** 331–351.
Zak, A. R. and Williams, M. L. (1963). Crack point stress singularities at a bi-material interface. *J. Appl. Mech.* **30,** 142.
Zwiers, R. I., Ting, T. C. T. and Spilker, R. L. (1982). On the logarithmic singularity of free-edge stress in laminated composites under uniform extension. *J. Appl. Mech.* **49,** 561–569.

APPENDIX

For the quartic eigenvalue problem:

$$(\lambda^4\mathbf{A}+\lambda^3\mathbf{B}+\lambda^2\mathbf{C}+\lambda\mathbf{D}+\mathbf{E})\mathbf{x}=0. \tag{A.1}$$

If **A** is nonsingular it is possible to transform the above quartic eigenvalue problem to the form:

$$(-\lambda^3\mathbf{A}^{-1}\mathbf{B}-\lambda^2\mathbf{A}^{-1}\mathbf{C}-\lambda\mathbf{A}^{-1}\mathbf{D}-\mathbf{A}^{-1}\mathbf{E})\mathbf{x}=\lambda^4\mathbf{x}, \tag{A.2}$$

or:

$$-\mathbf{A}^{-1}\mathbf{B}\mathbf{u}-\mathbf{A}^{-1}\mathbf{C}\mathbf{z}-\mathbf{A}^{-1}\mathbf{D}\mathbf{y}-\mathbf{A}^{-1}\mathbf{E}\mathbf{x}=\lambda\mathbf{u}, \tag{A.3}$$

$$\mathbf{y}=\lambda\mathbf{x}, \tag{A.4}$$

$$\mathbf{z}=\lambda\mathbf{y}, \tag{A.5}$$

$$\mathbf{u}=\lambda\mathbf{z}. \tag{A.6}$$

Equations (A.3)–(A.6) can be specified in a standard eigenvalue form as:

$$\begin{bmatrix} -\mathbf{A}^{-1}\mathbf{B} & -\mathbf{A}^{-1}\mathbf{C} & -\mathbf{A}^{-1}\mathbf{D} & -\mathbf{A}^{-1}\mathbf{E} \\ \mathbf{I} & \mathbf{0} & \mathbf{0} & \mathbf{0} \\ \mathbf{0} & \mathbf{I} & \mathbf{0} & \mathbf{0} \\ \mathbf{0} & \mathbf{0} & \mathbf{I} & \mathbf{0} \end{bmatrix} \begin{Bmatrix} \mathbf{u} \\ \mathbf{z} \\ \mathbf{y} \\ \mathbf{x} \end{Bmatrix} = \lambda \begin{Bmatrix} \mathbf{u} \\ \mathbf{z} \\ \mathbf{y} \\ \mathbf{x} \end{Bmatrix}. \tag{A.7}$$

Furthermore, the roles of **A** and **E** may be reversed if $\mu = 1/\lambda$ is substituted for λ. If both **A** and **E** are singular, an alternative reduction can be used by transforming the equations to the parameter μ, where:

$$\mu=\frac{\theta+\lambda}{\theta-\lambda}, \tag{A.8}$$

in this case $\lambda = \theta(\mu-1)/(\mu+1)$, giving:

$$(\mu^4\mathbf{A}^*+\mu^3\mathbf{B}^*+\mu^2\mathbf{C}^*+\mu\mathbf{D}^*+\mathbf{E}^*)\mathbf{x}=0, \tag{A.9}$$

where

$$\mathbf{A}^*=\theta^4\mathbf{A}+\theta^3\mathbf{B}+\theta^2\mathbf{C}+\theta\mathbf{D}+\mathbf{E}, \tag{A.10}$$

$$\mathbf{B}^*=-4\theta^4\mathbf{A}-2\theta^3\mathbf{B}+2\theta\mathbf{D}+4\mathbf{E}, \tag{A.11}$$

$$\mathbf{C}^*=6\theta^4\mathbf{A}-2\theta^2\mathbf{C}+6\mathbf{E}, \tag{A.12}$$

$$\mathbf{D}^*=-4\theta^4\mathbf{A}+2\theta^3\mathbf{B}-2\theta\mathbf{D}+4\mathbf{E}, \tag{A.13}$$

$$\mathbf{E}^*=\theta^4\mathbf{A}-\theta^3\mathbf{B}+\theta^2\mathbf{C}-\theta\mathbf{D}+\mathbf{E}. \tag{A.14}$$

The parameter θ may be used to regulate the relative magnitudes of the contributions of **A**, **B**, **C**, **D** and **E** to $\mathbf{A}^*$. The suitable θ will be chosen so that $\mathbf{A}^*$ is nonsingular.

For the quadratic eigenvalue problem [see eqn (31)]:

$$(\lambda^2\mathbf{A}+\lambda\mathbf{B}+\mathbf{C})\mathbf{x}=0, \tag{A.15}$$

if **A** is nonsingular, it can be converted to the standard form:

$$\begin{bmatrix} -\mathbf{A}^{-1}\mathbf{B} & -\mathbf{A}^{-1}\mathbf{C} \\ \mathbf{I} & \mathbf{0} \end{bmatrix} \begin{Bmatrix} \mathbf{y} \\ \mathbf{x} \end{Bmatrix} = \lambda \begin{Bmatrix} \mathbf{y} \\ \mathbf{x} \end{Bmatrix}, \tag{A.16}$$

if both **A** and **C** are singular, let $\mu = (\theta+\lambda)/(\theta-\lambda)$, and equation A.15 becomes:

$$(\mu^2\mathbf{A}^*+\mu\mathbf{B}^*+\mathbf{C}^*)\mathbf{x}=0, \tag{A.17}$$

where

$$\mathbf{A}^*=\theta^2\mathbf{A}+\theta\mathbf{B}+\mathbf{C};\quad \mathbf{B}^*=-2\theta^2\mathbf{A}+2\mathbf{C};\quad \mathbf{C}^*=\theta^2\mathbf{A}-\theta\mathbf{B}+\mathbf{C}. \tag{A.18}$$